UNIVERSITY OF LEEDS

This is a repository copy of *Latest Wuchiapingian to Earliest Triassic Conodont Zones and δ13Ccarb Isotope Excursions from Deep-Water Sections in Western Hubei Province, South China*.

White Rose Research Online URL for this paper:
http://eprints.whiterose.ac.uk/152921/

Version: Accepted Version

Article:

Yang, B, Li, H, Wignall, PB orcid.org/0000-0003-0074-9129 et al. (5 more authors) (2019) Latest Wuchiapingian to Earliest Triassic Conodont Zones and δ13Ccarb Isotope Excursions from Deep-Water Sections in Western Hubei Province, South China. Journal of Earth Science, 30 (5). pp. 1059-1074. ISSN 1674-487X

https://doi.org/10.1007/s12583-019-1018-2

© 2019, China University of Geosciences (Wuhan) and Springer-Verlag GmbH Germany, Part of Springer Nature. This is an author produced version of a paper published in Journal of Earth Science. Uploaded in accordance with the publisher's self-archiving policy.

Reuse
Items deposited in White Rose Research Online are protected by copyright, with all rights reserved unless indicated otherwise. They may be downloaded and/or printed for private study, or other acts as permitted by national copyright laws. The publisher or other rights holders may allow further reproduction and re-use of the full text version. This is indicated by the licence information on the White Rose Research Online record for the item.

Takedown
If you consider content in White Rose Research Online to be in breach of UK law, please notify us by emailing eprints@whiterose.ac.uk including the URL of the record and the reason for the withdrawal request.

White Rose
university consortium
Universities of Leeds, Sheffield & York

eprints@whiterose.ac.uk
https://eprints.whiterose.ac.uk/

Latest Wuchiapingian to earliest Triassic conodont zones and $\delta^{13}C_{carb}$ isotope excursions from deep-water sections in western Hubei Province, South China

Bo Yang[1,2], Hanxiao Li[1], Paul B. Wignall[3], Haishui Jiang[1,4], Zhijun Niu[2], Qian Ye[5], Qiong Wu[6], Xulong Lai[1,4*]

1. School of Earth Sciences, China University of Geosciences, Wuhan, Hubei 430074, China
2. Wuhan Center of Geological Survey, Guanggu Road 69, Wuhan, Hubei 430074, China
3. School of Earth & Environment, University of Leeds, Leeds, LS2 9JT, UK
4. State Laboratory of Geobiology and Environmental Geology, China University of Geosciences, Wuhan, Hubei 430074, China
5. Non-ferrous Metals Geological Exploration Bureau of Zhejiang Province,160 Renmin Middle Road, Shaoxing, Zhejiang 312000, China
6. State Laboratory of Palaeontology and Stratigraphy, Nanjing Institute of Geology and Palaeontology, 39 East Beijing Road, Nanjing 210008, China

*Corresponding author: xllai@cug.edu.cn

Bo Yang: https://orcid.org/0000-0003-2234-9492

Xulong Lai: https://orcid.org/0000-0002-2837-0885

ABSTRACT: Deep-water facies sections have advantages of recording complete information across the Permian-Triassic boundary (PTB). Here we present a detailed study on the conodont biostratigraphy and carbon isotope profile ranges from the Wuchiapingian-Changhsingian boundary (WCB) to the PTB of two deep-water facies sections at Zhuqiao and Shiligou in the Middle Yangtze region, western Hubei, South China. Fifteen species and three genera are identified. Eight conodont zones are recognized, in ascending order, they are the Clarkina orientalis, C. wangi, C. subcarinata, C. changxingensis, C. yini, C. meishanensis, Hindeodus parvus and Isarcicella isarcica Zones. The onset of deposition of the deep-water siliceous strata of the Dalong Formation in western Hubei began in the late Wuchiapingian and persisted to the late Changhsingian. Carbon isotope negative excursions occur near both the WCB and PTB in both sections. The WCB $\delta^{13}C_{carb}$ negative excursion is in the C. orientalis and C. wangi zones. The PTB $\delta^{13}C_{carb}$ negative excursion began in the C. yini Zone and extended to the I. isarcica Zone. The absence of several Changhsingian zones may indicate the difficulty of extracting conodonts from siliceous strata or the presence of an intra-Changhsingian hiatus.

KEY WORDS: Dalong Formation, conodonts, $\delta^{13}C_{carb}$ isotope, Wuchiapingian-Changhsingian boundary, Permian-Triassic boundary

0 INTRODUCTION

The end-Permian saw the largest mass extinction in history with 95% of marine species and 75% of terrestrial species disappearing (Shen and Bowring, 2014; Erwin, 2006; Benton and Twitchett, 2003; Jin et al., 2000; Raup and Sepkoski, 1982; Sepkoski, 1981). In contrast, the losses of conodont were relatively moderate, they are more likely to record some effectively information about Permian-Triassic mass extinction compared with other contemporaneous organisms (Lai et al., 2018). Conodont plays an important role in constructing biostratigraphic framework during this period. For example, the first appearance of Hindeodus parvus is the marker for the base of Early Triassic (Yin et al., 2001), and some key conodonts could be used to establish conodont zones and make global comparison (e.g. Lyu et al., 2019; Kolar-Jurkovšek et al., 2018; Brosse et al., 2017; Wang et al., 2017; Jiang et al., 2014, 2011, 2007; Yuan et al., 2014; Zhang et al., 2014; Yang et al., 2012; Metcalfe et al., 2008; Zhao et al., 2007; Perri and Farabegoli, 2003). Especially, a high-resolution conodont zonation across the PTB has been reported at the Meishan section, South China (Chen et al., 2015; Yuan et al., 2014; Zhang et al., 2009; Jiang et al., 2007). Based on the conodont biostratigraphy, the timing of the PTB mass extinction has been constrained from the top part of C. yini Zone to the I. staeschei Zone in Meishan (Song et al., 2013; Shen et al., 2011; Yin et al., 2007; Jin et al., 2000). Moreover, the conodont fauna was sensitive to palaeoenvironmental and climatic changes during the PTB period, which has been confirmed by the studies of conodont size variation (Chen et al., 2015; Schaal et al., 2015; Luo et al., 2006). Furthermore, conodont oxygen isotope has become a valuable tool for reconstructing sea-surface temperatures curve in the PTB interval, and a major temperature rise form the latest Permian to the Early Triassic has been reported (Schobben et al., 2014; Joachimski et al., 2012; Sun et al., 2012).

South China, with its well exposed PTB strata in the Yangtze region, remains one of the best studied regions (Lai et al., 2018; Yin et al., 2014). However, the conodont occurrences in the deep-water, basinal facies of western Hubei area, located in the Middle Yangtze region, are amongst the least studied in South China. A few works on Changhsingian conodont biostratigraphy have been documented at Ganxi (Lyu et al., 2019; Nafi et al., 2006) and Tianqiao (Wang and Xia, 2004a) in Xuanen County. Conodonts from the PTB and Early Triassic have been reported from Jianshi, Enshi City (Lyu et al., 2019) and Xiakou, Xingshan County (Zhao et al., 2013; Wang and Xia, 2004b) in western Hubei area.

Basinal sections have the advantage of recording more complete information across the PTB (Lai et al., 2018; Jiang et al., 2015; Yin et al., 2014), whilst most documented sections are in shallow-water, carbonate platform facies (Bai et al., 2017; Liang et al., 2016; Jiang et al., 2014; 2007; Chen et al., 2009; Tong and Zhao, 2005; Yin et al., 2001). Reports of conodonts from deep-water, bedded siliceous rocks are rare and restricted to reports from Dongpan in Guangxi (Luo et al., 2008) and Xinmin in Guizhou (Zhang et al., 2014).

Here we present a detailed study on the latest Wuchiapingian to earliest Triassic conodont biostratigraphy and carbon isotope profile from the deep-water basin facies of the Zhuqiao and Shiligou sections in the Middle Yangtze region of western Hubei, South China.

1 GEOLOGICAL SETTING

In South China, during the Changhsingian (Late Permian), the Middle Yangtze Block was mostly carbonate platform (Fig.1c), whilst siliceous strata of the Dalong Formation accumulated in deep-water on the northern and southwest margin of the Block (Yin et al., 2014; Feng and Gu, 2002). Contemporaneously, the western Hubei Basin was a large rift basin that formed an embayment in the northwestern margin of the Middle Yangtze Block (Liu et al., 2019; Zhuo et al., 2009) (Figs. 1a and 1b). The Zhuqiao and Shiligou sections were located in the western Hubei Basin during the PTB (Fig.1a). The Dalong Formation occurs extensively in western Hubei, and is considered a record of deep-water basin and deeper-water slope environments during the latest Permian (He et al., 2013). There are three sedimentary types of the Dalong Formation in this area from west to east, and they are siliceous rock to limestone and mudstone type, mudstone to siliceous rock type and siliceous limestone to mudstone type (Niu et al., 2000). The first two types are of deep-water, basin origin, whereas the last type is a transitional type between the basin and platform facies.

The Zhuqiao section is located next to the Zhuqiao hydropower station, 2 Km north of Zhuqiao village, Wufeng County, Yichang City, western Hubei Province, South China (Fig. 2). The exposed strata at the Zhuqiao section include the Late Permian Wuchiaping and Dalong formations, and the Early Triassic Daye Formation (Fig. 3). The top of Wuchiaping Formation is composed of grey, dolomitic limestone with bed thicknesses of more than 1 m. The Dalong Formation consists of grey to dark grey thin-bedded siliceous mudstone and carbonaceous mudstone with a few interbeds of dark grey medium- to thin-bedded limestone, forming rhythmic stratification, and with well-developed thin laminations. Planktonic or nektonic fossils including ammonoids and radiolarians are common in the thin-bedded siliceous mudstone. Thus, predominately siliceous facies of the Dalong Formation at Zhuqiao are considered a deep-water basin facies and belong to the mudstone to siliceous rock type of Niu et al. (2000). The Daye Formation consists of mudstone and muddy limestone with thin-bedded claystone.

The Shiligou section is located in Xinglong Town, Fengjie County of Chongqing City, along the roadside of the "Tourism Circle Way" (Fig. 2). The strata at Shiligou belong to the western Hubei Basin and consist of the well exposed Dalong and Daye formations (Fig. 3). The lower part of Dalong Formation is grey to black, thin-bedded siliceous mudstone and calcareous mudstone, similar to the Zhuqiao section, whereas the middle and upper parts consist of grey, medium- to thin-bedded limestone with calcareous mudstone interbedded. The Dalong Formation of the Shiligou section is also a deep-water, basinal facies and belongs to the siliceous rock to limestone and mudstone type of Niu et al. (2000). The overlying Daye Formation is composed of grey, thin-bedded limestone with interbedded mudstone.

2 MATERIALS AND METHODS

A total of 42 and 28 conodont samples (about 3-5 kg per sample) were collected from the Dalong and Daye formations at Zhuqiao and Shiligou respectively. Limestone samples were processed by dilute acetic acid (10%) (Jiang et al., 2007), mudstone samples were cracked by dithionite solution and hydrogen peroxide, and siliceous mudstone samples were dissolved by dilute hydrofluoric acid (5%). LST-an inorganic heavy liquid was used in conodont separation as described by Yuan et al. (2015). Fifteen species belonging to three genera (Clarkina, Hindeodus and Isarcicella) of conodont P_1 elements were identified (1553 from the Zhuqiao section and 91 from the Shiligou section), and some key species are illustrated in Plate 1 to 4.

For $\delta^{13}C_{carb}$ and $\delta^{18}O$ measurement, 106 and 60 fresh, whole rock samples were taken from the Zhuqiao and Shiligou sections respectively. Weathered surfaces and large calcite veins were avoided, and all samples were crushed to less than 200 meshes with a dentist drill. Analysis was conducted at the State Key Laboratory of Biogeology and Environmental Geology, China University of Geosciences (Wuhan) with a MAT-253 mass spectrometer with standard methodology (see Supplemental data).

A positive correlation between $\delta^{13}C_{carb}$ and $\delta^{18}O_{carb}$ is usually explained as a sign of the influence of meteoric diagenesis (Meyers and Lohmann, 1985). Most of the $\delta^{18}O_{carb}$ values obtained from Dalong Formation in our sections range from -4.0‰ to -8.0‰, indicating a weak influence of meteoric diagenesis. This conclusion is supported by the finding of the weak correlation ($R^2=10^{-4}$ and 10^{-2}) between $\delta^{13}C_{carb}$ and $\delta^{18}O_{carb}$ (see Supplemental data).

3 CONODONT BIOSTRATIGRAPHY

A total of eight conodont zones have been identified indicating ages ranging from the latest Wuchiapingian to earliest Triassic from the two sections in the western Hubei area. In ascending order, they are the C. orientalis in the latest Wuchiapingian, C. wangi, C. subcarinata, C.

changxingensis, C. yini and C. meishanensis zones in the Changhsingian, H. parvus and I. isarcica zones in the Griesbachian. The Zhuqiao section has the C. orientalis, C. wangi, C. meishanensis, H. parvus and I. isarcica zones, whilst the Shiligou section has the C. orientalis, C. wangi, C. subcarinata, C. changxingensis and C. yini zones.

3.1 Clarkina orientalis Zone

This zone is discovered at both Zhuqiao (0-10.85 m, beds 1-24) and Shiligou (0-7.24 m, beds1-6) (Figs. 4 and 5). The lower limit of this zone is undefined because there was no sampling below this level. The upper limit is defined by the first occurrence (FO) of C. wangi. C. orientalis is the dominant species in this zone, especially abundant at the Zhuqiao section, where it occurs in most of the lower part of Dalong Formation. Besides the zonal conodont, only a few C. guangyuanensis, C. transcaucasica and C. liangshanensis were found in sample ZQC-1 at Zhuqiao.

The C. orientalis Zone was first established by Kozur (1975) in Archura, Transcaucasia and is widely known in South China (Shen and Mei, 2010; Shen et al., 2007; Jin et al., 2006; Nafi et al., 2006; Mei et al., 1994) and Iran (Shen and Mei, 2010; Yazdi and Shirani, 2002). Though the range of C. orientalis could extend into the C. wangi Zone of basal Changhsingian, Shen (2007) particularly researched the spatial and temporal distribution of C. orientalis and showed that populations of this species are a distinct late Wuchiapingian maker. The base of C. orientalis Zone at the Zhuqiao and Shiligou sections are undefined, but this zone can be correlated with the Neogondolella orientalis-N. longicuspidata Zone and C. longicuspidata Zone at the Meishan section (Yuan et al., 2014; Zhang et al., 2009), Ganxi section (Nafi et al., 2006) and Shangsi section (Shen et al., 2013) in South China and the C. orientalis Zone established by Shen and Mei (2010) in Iran. The age of this zone is late Wuchiapingian.

3.2 Clarkina wangi Zone

This zone is identified at both Zhuqiao (10.85-10.96 m, bed 25a) and Shiligou (7.24-11.39 m, beds 6-8) (Figs. 4 and 5). Lower limit: the first occurrence of C. wangi. The upper limit of this zone at the Shiligou section is defined by the first occurrence of C. subcarinata. However, at the Zhuqiao section, the upper limit is defined by the first occurrence of C. meishanensis in bed 25b. Associated conodonts are C. orientalis and C. sp.. C. wangi has its maximal abundance in the C. wangi Zone, especially in Zhuqiao, and we found hundreds of C. wangi specimens.

Mei and Henderson (2001) first established the C. wangi-C. subcarinata Zone at the Meishan section and C. wangi had not been discovered outside South China at that time. Because the lower part of the zone is dominated by C. wangi, Mei et al. (2004) subsequently distinguished a C. wangi Zone from the C. wangi-C. subcarinata Zone. The Global Stratotype Section and Point (GSSP) for the basial boundary of the Changhsingian Stage was then defined at the first appearance datum of the conodont C. wangi within the C. longicuspidata to C.wangi lineage by Jin et al. (2006).

3.3 Clarkina subcarinata Zone

This early Changhsingian zone is only recognized in the Shiligou section (11.39-28.14m, beds8-12) (Fig. 5). Lower limit: the first occurrence of C. subcarinata, upper limit: the first occurrence of C. changxingensis. Associated conodonts are C. orientalis, C. wangi, and C. sp.. This zone has been widely studied around the world (Yuan et al., 2014; Shen and Mei, 2010; Ji et al., 2007; Kozur, 2005, 2004). Nafi et al. (2006) failed to differentiate this zone from the C. wangi Zone at their Ganxi section. The C. wangi Zone of Ganxi actually consists of both the C. wangi and C. subcarinata zones. This zone at Shiligou is equivalent to the C. subcarinata Zone of

Meishan (Yuan et al., 2014) and Shangsi (Yuan et al., 2019; Shen et al., 2013) and sections in Iran (Shen and Mei, 2010).

3.4 Clarkina changxingensis Zone

This middle Changhsingian zone has only been identified in the Shiligou section (28.14-31.64 m, beds 12-15) (Fig. 5). Lower limit: the first occurrence of C. changxingensis, upper limit: the first occurrence of C. yini. Associated conodonts are C. deflecta and C. sp.. Wang and Wang (1981) first established the C. deflecta-C. changxingensis assemblage Zone at the Meishan section in South China, and the C. changxingensis Zone was since been widely reported around Paleotethys (Lyu et al., 2019; Bai et al., 2017; Yuan et al., 2014; Zhang et al., 2014; Shen and Mei, 2010; Zhang et al., 2009; Nafi et al., 2006; Mei et al., 1998; Orchard and Krystyn, 1998). The C. changxingensis Zone of the Shiligou section is equivalent to the middle and upper parts of the Neogondolella changxingensis-N. deflecta Zone of Zhang et al. (2009), and the C. changxingensis Zone of Yuan et al. (2014) at the Meishan section.

3.5 Clarkina yini Zone

This late Changhsingian zone is only found at Shiligou (31.64-35.39 m, bed 15-16) (Fig. 5). Lower limit: the first occurrence of C. changxingensis, although we only found a few C. changxingensis and C. yini individuals in bed 15 and 16 at Shiligou. And abundant Early Triassic bivalve Claraia and ammonoid Ophiceras are found in the bottom of bed 17, we put the upper limit of this zone in the uppermost part of bed 16. It is largely equivalent to the Neogondolella yini Zone at the Meishan (Jiang et al., 2007) and Shangsi sections (Jiang et al., 2011), and the C. yini Zone of the Ganxi section (Nafi et al., 2006).

3.6 Clarkina meishanensis Zone

This late Changhsingian zone is only identified at Zhuqiao (10.96-11.01m, beds 25b) (Fig. 5). Lower limit: the first occurrence of C. meishanensis, upper limit is placed at the top of bed 25b. No conodont species were found from bed 25c to bed 27, wo could not identify any zone in this interval. Just a few C. meishanensis were found in this zone and preserved badly, because a dithionite solution and hydrogen peroxide were used to crack the black mudstone of samples for conodont extraction. This zone was first established by Mei et al. (1998) at the Meishan section. The C. meishanensis of the Meishan section is in bed 25b of dark gray clay. The C. meishanensis at the Zhuqiao section may be equivalent to the Neogondolella meishanensis zone at Meishan (Jiang et al., 2007).

3.7 Hindeodus parvus Zone

This zone is only discovered at Zhuqiao (12.15-12.8m, beds28-30) (Fig. 4). Lower limit: the first occurrence of H. parvus. Upper limit: the first occurrence of Isarcicella isarcica. Associated taxa: C. orchard, H. sp., and C. sp.. The First Appearance Datum of H. parvus was used to defined the GSSP for the basal boundary of the Triassic System by Yin et al. (2001), and it has been widely used since (e.g. Lyu et al., 2019; Bai et al., 2017; Yuan et al., 2014; Zhang et al., 2014; Zhao et al., 2013; Jiang et al., 2007; Perri and Farabegoli, 2003). However, the first occurrence of H. parvus in our study was in bed 28, 0.36m higher than the first occurrence of Ophiceras in bed 27, which we use to define the beginning of the Triassic in our section.

We have not found H. parvus in the Shiligou section, but abundant Early Triassic Claraia and and Ophiceras were found in the bottom of bed 17. Furthermore, we found H. aff. parvus (Pl. 4, fig. 21) from Sample SLG-17C3 in bed 17. So, we consider the age of bed 17 at the Shiligou section to be the Earliest Triassic.

3.8 Isarcicella isarcica Zone

This mid Griesbachian zone is only found in the Zhuqiao section (12.8-13.96m, beds30-34)

(Fig. 4). Lower limit: the first occurrence of Isarcicella isarcica. Upper limit is uncertain, because no samples were taken from above bed 34. Associated taxa: H. parvus and H. sp.. I. isarcica was first obtained by Huckriede (1958) in northern Italy. The I. isarcica Zone usually overlies the I. staeschei Zone (Zhang et al., 2014; Zhao et al., 2013; Jiang et al., 2007). However, we failed to establish this zone at Zhuqiao, where the I. isarcica Zone of the Zhuqiao section is believed to correspond to I. isarcica Zone at Meishan (Jiang et al., 2007) and Daxiakou (Zhao et al., 2013).

4 CARBON ISOTOPE STRATIGRAPHY

Carbon isotope variations in the PTB interval show a rapid and large negative excursions in both $\delta^{13}C_{carb}$ and $\delta^{13}C_{org}$ records and provide an age control independent of conodont stratigraphy (e.g. Shen et al., 2013; Song et al., 2012; Korte and Kozur, 2010; Xie et al., 2007). The carbon isotope excursion around the WCB is also well documented in South China (e.g. Wei et al., 2015; Shen et al., 2013; Jin et al., 2006; Shao et al., 2000). However, whether the $\delta^{13}C$ excursion across the WCB is a global event or a special phenomenon influenced by regional factors is still unknown. Shao et al. (2000) documented a $\delta^{13}C$ anomaly at the WCB in Guizhou and Guangxi of South China, and considered this WCB excursion to be a global negative carbon isotopic excursion because more ^{12}C-rich CO_2 was released into the atmosphere. Shen et al. (2010) documented that the negative excursion around the WCB showed different magnitudes and patterns, and proposed that whether this excursion is due to local or global controls still remain unresolved. Wei et al. (2015) considered the significant negative excursion at the WCB was probably a global signal and mainly caused by the low primary productivity. Liao et al. (2016) suggested that the change in sedimentary environment had an important influence on the $\delta^{13}C$ values across the WCB. Here, we document carbon isotope data from WCB to PTB at the Zhuqiao and Shiligou sections (Fig. 6).

At Zhuqiao, the $\delta^{13}C_{carb}$ profile shows a gradual negative decline in the C. orientalis Zone with the values beginning to decline from 0.41‰ at 3.77m in bed 7 to the minimum -2.85‰ at 9.96m in bed 22, followed by the brief positive peak between +0.51‰ and +0.84‰ around the WCB. The negative $\delta^{13}C_{carb}$ excursion near the PTB is also showed. The excursion shows a negative excursion trend form the C. meishanensis Zone to I. isarcica Zone with the average -0.75‰. The $\delta^{13}C_{carb}$ values are variable around the PTB, and can not be compared with the Meishan section (Shen et al., 2013; Xie et al., 2007) and other section in South China (Yuan et al., 2015; Shen et al., 2013), which is difficult to explain. It seems there are some noises of the carbon isotope excursion at the PTB of Zhuqiao, the carbonate dolomitization is obvious near the PTB of Zhuqiao section (Fig.3 b), the carbonate dolomitization maybe one possible explanation.

The $\delta^{13}C_{carb}$ data should show a clear negative excursion across the WCB at Shiligou. The $\delta^{13}C_{carb}$ curve indicates a negative excursion trend in the C. orientalis Zone and C. wangi Zone with the average -0.85‰, then the rapid recovery to stable values with the average value 0.64‰ from the C. subcarinata to the C. yini zones. The negative excursion around the PTB is more clearly observed at Shiligou. The $\delta^{13}C_{carb}$ values are stable during the most part of Changhsingian with the average +0.64‰ from the C. subcarinata Zone to the C. yini Zone, which are consistent with the $\delta^{13}C_{carb}$ values in the Changhsingian of many other sections (Shen et al., 2013). The $\delta^{13}C_{carb}$ values begins to gradually decline at the base of C. yini Zone from 0.92‰ to -0.01‰, followed by a sharp negative shift 3.62‰ from 0.81‰ to -2.81‰ in the upper part of C. yini Zone, which may compare with the sharp 5‰ decline within the C. meishanensis Zone at the Meishan section (Xie et al., 2007). Above the PTB, the $\delta^{13}C_{carb}$ values are stable on the average -0.80‰ in bed 17.

5 DISCUSSION

5.1 Definition of the Wuchiapingian-Changhsingian Boundary

The Global Stratotype Section and Point (GSSP) for the base of the Changhsingian Stage was defined at the First Appearance Datum of the conodont C. wangi within the lineage from C. longicuspidata to C.wangi (Jin et al., 2006). C. wangi occurs in both the Zhuqiao and Shiligou sections, with the C. orientalis zone below. We suggest that the WCB of the Zhuqiao section should be placed at 10.85m in the base of bed 25a and the WCB of Shiligou section should be laid at 7.24m in the lower of bed 6.

5.2 Definition of the Permian-Triassic Boundary

At the Zhuqiao section, the first occurrence of H. parvus is in bed 28 which is 0.36 m higher than the first occurrence of Ophiceras (Figs. 3b and 3c) in bed 27. We define the PTB of the Zhuqiao section by the first occurrence of Ophiceras in bed 27(11.74 m), which is 0.36 m below the first occurrence of H. parvus.

H. parvus is not found at Shiligou, but abundant Early Triassic Claraia and Ophiceras are found in bed 17 instead, where H. aff. parvus also occurs. So, we consider the age of bed 17 at Shiligou section should be the Earliest Triassic. Taking the negative excursion around the PTB from the Shiligou section into account, we suggest the PTB of the Shiligou section is at 35.39m, which is the bottom of bed 17.

5.3 The temporal and spatial distribution of Dalong Formation in western Hubei

In South China, chert deposition in the Dalong Formation has been found to persist into the earliest Triassic in the Gaimao (Yang et al., 2012) and Xinmin sections (Zhang et al., 2014) of Guizhou Province, although generally this unit is considered to record latest Permian siliceous sedimentation in deep-water basin and slope environments (He et al., 2013; Chen et al., 2010).

Since the definition of Dalong Formation was confirmed by Zhao et al. (1978), the Dalong Formation in western Hubei area is usually considered to be of a Changhsingian age (He et al., 2013), although the ammonoids recorded by Niu et al. (2000) indicate a Late Wuchiapingian to Changhsingian age. Our conodont studies at Zhuqiao and Shiligou confirm this age range.

Three conodont zones (C. subcarinata, C. changxingensis and C. yini Zones) are absent from the Dalong Formation at the Zhuqiao section between the C. wangi Zone and C. meishanensis Zone. This may partly reflect the difficulty of extracting conodonts from siliceous strata that dominate this section. Previously reported conodont studies at siliceous-dominated sections at Dongpan (Luo et al., 2008) and Xinmin (Zhang et al., 2014) also show that the conodont zones in both sections are not complete. If this reason is right, the three missing zones are supposed be within the C. orientalis Zone, and further research is needed to differentiate them from the C. orientalis Zone. Alternatively, the absence could be due to a hiatus, possibly be between bed 24 and 25a at the Zhuqiao section. Evidences for this hiatus is: 1. a sudden change of lithology between beds 24 and bed 25a from siliceous mudrock to limestone, 2. the surface of limestone in bed 25a is irregular (Fig. 3d), 3. $\delta^{13}C_{carb}$ values show an increase at 24/25a boundary. If this reason is correct, the hiatus in Zhuqiao section may be caused by a regional regression, which is potentially attributed to the regional crustal uplift which should begin from the south to north in the Western Hubei Basin, as a result the Shiligou section is almost unaffected and with no conodont zone absent. During the Late Permian, the western Hubei Basin was a longitudinal tensile depression rift basin with many faults, especially in the east, which may cause a regional crustal uplift (Zhuo et al., 2009).

6 CONCLUSIONS

Fifteen species belonging to three genera (Clarkina, Hindeodus and Isarcicella) of conodont

P_1 elements were identified and eight conodont zones are recognized from the Dalong to the lower Daye Formations at the Zhuqiao and Shiligou sections near the western Hubei Province, South China. In ascending order, they are C. orientalis, C. wangi, C. subcarnata, C. changxingensis, C. yini, C. meishanensis, H. parvus and I. isarcica zones. Several zones are missing from the Changhsingian (C. subcarinata, C. changxingensis and C. yini Zones) either due to collection failure or the presence of a hiatus.

There are both carbon isotope negative excursions occur near the WCB and PTB at the Zhuqiao section and Shiligou section. The WCB $\delta^{13}C_{carb}$ negative excursion is in the C. orientalis zone at the Zhuqiao section with the average -1.08‰, follow by the brief positive peak between +0.51‰ and +0.84‰ around the WCB. At the Shiligou section, the WCB $\delta^{13}C_{carb}$ negative excursion occurs in the C. orientalis and the C. wangi zones, then there is a rapid recovery to stable values with the average value 0.64‰ from the C. subcarinata to the C. yini zones. The PTB $\delta^{13}C_{carb}$ negative excursions are also showed. At Zhuqiao, the negative excursion ranges from the C. meishanensis Zone to the I. isarcica Zone. At Shiligou, the PTB $\delta^{13}C_{carb}$ values begin to gradual decline at the base of C.yini Zone, with a sharp negative shift 3.62‰ in the upper part of C. yini Zone, followed by a stable negative values on the average -0.80‰ during the Early Triassic.

On Basis of conodont zones and carbon isotope data, the WCB of the Zhuqiao section is placed at 10.85 m in the base of bed 25a and the WCB of the Shiligou section should be laid at 7.24 m in the lower of bed 6, meanwhile, the PTB of the Zhuqiao section is drawn at 11.74 m in bed 27 and the PTB of the Shiligou section is placed at 35.39 m in the bottom of bed 17.

ACKNOWLEDGMENT(S)

This work was supported by the Natural Science Foundation of China (grants nos. 41572002, 41830320, 41272044, 41472087, 4183000426). All thanks are due to Zaitian Zhang, Chunbo Yan, Rong Chen and Lina Wang for their help in field sampling. All SEM pictures were undertaken at the State Key Laboratory of Biogeology and Environmental Geology, China University of Geosciences (Wuhan). Finally，we thank the two anonymous reviewers for their constructive suggestions.

REFERENCES CITED

Bai, R., Dai, X. ,Song, H., 2017. Conodont and Ammonoid Biostratigraphies around the Permian-Triassic Boundary from the Jianzishan of South China. Journal of Earth Science, 28(4): 595-613. https://doi.org/510.1007/s12583-12017-10754-12584

Benton, M. J. ,Twitchett, R. J., 2003. How to kill (almost) all life: the end-Permian extinction event. Trends in Ecology & Evolution, 18(7): 358-365. https://doi.org/310.1016/s0169-5347(1003)00093-00094

Brosse, M., Baud, A., Bhat, G. M., et al., 2017. Conodont-based Griesbachian biochronology of the Guryul Ravine section (basal Triassic, Kashmir, India). Geobios, 50(5): 359-387. https://doi.org/310.1016/j.geobios.2017.1010.1001

Chen, J., Beatty, T. W., Henderson, C. M., et al., 2009. Conodont biostratigraphy across the Permian-Triassic boundary at the Dawen section, Great Bank of Guizhou, Guizhou Province, South China: Implications for the Late Permian extinction and correlation with Meishan. Journal of Asian Earth Sciences, 36(6): 442-458. https://doi.org/410.1016/j.jseaes.2008.1008.1002

Chen, Y., Jiang, H., Lai, X., et al., 2015. Early Triassic conodonts of Jiarong, Nanpanjiang Basin, southern Guizhou Province, South China. Journal of Asian Earth Sciences, 105: 104-121. https://doi.org/10.1016/j.jseaes.2015.03.014

Chen, Y., Ye, Q., Jiang, H., et al., 2018. Conodonts and Carbon Isotopes during the Permian-Triassic Transition on the Napo Platform, South China. Journal of Earth Science. https://doi.org/10.1007/s12583-018-0884-3

Chen, Z., Tong, J., Liao, Z., et al., 2010. Structural changes of marine communities over the Permian-Triassic transition: Ecologically assessing the end-Permian mass extinction and its aftermath. Global and Planetary Change, 73(1): 123-140. https://doi.org/110.1016/j.gloplacha.2010.1003.1011

Chen, Z., Yang, H., Luo, M., et al., 2015. Complete biotic and sedimentary records of the Permian-Triassic transition from Meishan section, South China: Ecologically assessing mass extinction and its aftermath. Earth-Science Reviews, 149: 67-107. http://dx.doi.org/10.1016/j.earscirev.2014.10.005

Erwin, D. H., 2006. Extinction: How life on Earth nearly ended 250 million years ago. Biologist, 311(5769): 1868-1869

Feng, Q. ,Gu, S., 2002. Uppermost Changxingian (Permian) radiolarian fauna from southern Guizhou, Southwestern China. Journal of Paleontology, 76(5): 797-809. https://doi.org/710.1666/0022-3360(2002)1076<0797:ucprff>1662.1660.co;1662

Feng, Z., Bao, Z., Wu, S., et al., 1997. Lithofacies palaeogeography of the Early and Middle Triassic of South China. Chinese Journal of Geology, 32(2): 212-220. (in Chinese with English Abstract)

He, Y., Luo, J., Wen, Z., et al., 2013. Lithofacies palaeogeography of the Upper Permian Changxing Stage in the Middle and Upper Yangtze Region, China. Journal of Palaeogeography, 2(2): 139-162. https://doi.org/110.3724/SP.J.1261.2013.00023

Huckriede, R., 1958. Die Conodonten der mediterranen Trias und ihr stratigraphischer Wert. Paläontologische Zeitschrift, 32(3): 141-175. https://doi.org/110.1007/BF02989028

Ji, Z., Yao, J., Isozaki, Y., et al., 2007. Conodont biostratigraphy across the Permian-Triassic boundary at Chaotian, in Northern Sichuan, China. Palaeogeography, Palaeoclimatology, Palaeoecology, 252(1): 39-55. https://doi.org/10.1016/j.palaeo.2006.1011.1033

Jiang, H., Lai, X., Luo, G., et al., 2007. Restudy of conodont zonation and evolution across the P/T boundary at Meishan section, Changxing, Zhejiang, China. Global and Planetary Change, 55(1): 39-55. https://doi.org/10.1016/j.gloplacha.2006.1006.1007

Jiang, H., Lai, X., Yan, C., et al., 2011. Revised conodont zonation and conodont evolution across the Permian-Triassic boundary at the Shangsi section, Guangyuan, Sichuan, South China. Global and Planetary Change, 77(3–4): 103-115. https://doi.org/110.1016/j.gloplacha.2011.1004.1003

Jiang, H., Lai, X., Sun, Y., et al., 2014. Permian–Triassic Conodonts from Dajiang(Guizhou, South China) and Their Implication for the Age of Microbialite Deposition in the Aftermath of the End-Permian Mass Extinction. Journal of Earth Science, 25(3): 413-430. https://doi.org/410.1007/s12583-12014-10444-12584

Jiang, H., Joachimski, M. M., Wignall, P. B., et al., 2015. A delayed end-Permian extinction in deep-water locations and its relationship to temperature trends (Bianyang, Guizhou Province, South China). Palaeogeography, Palaeoclimatology, Palaeoecology, 440: 690-695. https://doi.org/610.1016/j.palaeo.2015.1010.1002

Jin, Y., Wang, Y., Wang, W., et al., 2000. Pattern of marine mass extinction near the Permian-Triassic boundary in South China. Science, 289(5478): 432-436. https://doi.org/410.1126/science.1289.5478.1432

Jin, Y., Wang, Y., Henderson, C., et al., 2006. The Global Boundary Stratotype Section and Point (GSSP) for the base of Changhsingian Stage (Upper Permian). Episodes, 29(3): 175-182

Kolar-Jurkovšek, T., Jurkovšek, B., Nestell, G. P., et al., 2018. Biostratigraphy and sedimentology of Upper Permian and Lower Triassic strata at Masore, western Slovenia. Palaeogeography, Palaeoclimatology, Palaeoecology, 490(Supplement C): 38-54. https://doi.org/10.1016/j.palaeo.2017.1009.1013

Korte, C. ,Kozur, H. W., 2010. Carbon-isotope stratigraphy across the Permian-Triassic boundary: A review. Journal of Asian Earth Sciences, 39(4): 215-235. https://doi.org/210.1016/j.jseaes.2010.1001.1005

Kozur, H. W., 1975. Beitrage zur Conodontenfauna des Perm. Geologische Und Palaontologische Mitteilungen Innsbruck, 5: 1-44

Kozur, H. W., 2004. Pelagic uppermost Permian and the Permian-Triassic boundary conodonts of Iran. Part 1:

Taxonomy. Hallesches Jahrbuch Fur Geowissenschaften, Reihe B: Geologie, Palaontologie, Mineralogie, 18: 39-68

Kozur, H. W., 2005. Pelagic uppermost Permian and the Permian-Triassic boundary conodonts of Iran. Part II: Investigated sections and evaluation of the conodont faunas. Hallesches Jahrbuch Fur Geowissenschaften, Reihe B: Geologie, Palaontologie,Mineralogie, 19: 49-86

Lai, X., Jiang, H. ,Wignall, P. B., 2018. A review of the Late Permian-Early Triassic conodont record and its significance for the end-Permian mass extinction. Revue de Micropaléontologie, 61(3): 155-164. https://doi.org/110.1016/j.revmic.2018.1010.1002

Liang, L., Tong, J., Song, H., et al., 2016. Lower-Middle Triassic conodont biostratigraphy of the Mingtang section, Nanpanjiang Basin, South China. Palaeogeography, Palaeoclimatology, Palaeoecology, 459: 381-393. https://doi.org/310.1016/j.palaeo.2016.1007.1027

Liao, Z., Hu, W., Cao, J., et al., 2016. Permian-Triassic boundary (PTB) in the Lower Yangtze Region, southeastern China: A new discovery of deep-water archive based on organic carbon isotopic and U–Pb geochronological studies. Palaeogeography, Palaeoclimatology, Palaeoecology, 451: 124-139. http://dx.doi.org/10.1016/j.palaeo.2016.03.004

Liu, W., Yao, J., Tong, J., et al., 2019. Organic matter accumulation on the Dalong Formation (Upper Permian) in western Hubei, South China: Constraints from multiple geochemical proxies and pyrite morphology. Palaeogeography, Palaeoclimatology, Palaeoecology, 514(15): 677-689. https://doi.org/610.1016/j.palaeo.2018.1011.1015

Luo, G., Lai, X., Jiang, H., et al., 2006. Size variation of the end Permian conodont Neogondolella at Meishan Section, Changxing, Zhejiang and its significance. Science in China Series D: Earth Sciences, 49(4): 337-347. https://doi.org/10.1007/s11430-006-0337-1

Luo, G., Lai, X., Feng, Q., et al., 2008. End-Permian conodont fauna from Dongpan section: Correlation between the deep-and shallow-water facies. Science in China Series D: Earth Sciences, 51(11): 1611-1622. https://doi.org/1610.1007/s11430-11008-10125-11431

Lyu, Z., Orchard, M. J., Chen, Z., et al., 2019. Uppermost Permian to Lower Triassic conodont successions from the Enshi area, western Hubei Province, South China. Palaeogeography, Palaeoclimatology, Palaeoecology, 519: 49-64.https://doi.org/10.1016/j.palaeo.2017.1008.1015

Mei, S., Jin, Y. ,Wardlaw, B. R., 1994. Succession of Wuchiapingian conodonts from Northeastern Sichuan and its worldwide correlation. Acta Micropalaeontologica Sinica, 11: 121-140

Mei, S., Zhang, K. ,Wardlaw, B. R., 1998. A refined succession of Changhsingian and Griesbachian neogondolellid conodonts from the Meishan section, candidate of the global stratotype section and point of the Permian-Triassic boundary. Palaeogeography, Palaeoclimatology, Palaeoecology, 143(4): 213-226. https://doi.org/210.1016/S0031-0182(1098)00112-00116

Mei, S. ,Henderson, C. M., 2001. Evolution of Permian conodont provincialism and its significance in global correlation and paleoclimate implication. Palaeogeography, Palaeoclimatology, Palaeoecology, 170(3): 237-260. https://doi.org/210.1016/S0031-0182(1001)00258-00259

Mei, S., Henderson, C. M. ,Cao, C., 2004. Conodont sample-population approach to defining the base of the Changhsingian Stage, Lopingian Series, Upper Permian. Geological Society London Special Publications, 230(1): 105-121. http://dx.doi.org/110.1144/GSL.SP.2004.1230.1101.1106

Metcalfe, I., Nicoll, R. S. ,Willink, R. J., 2008. Conodonts from the Permian-Triassic transition in Australia and position of the Permian-Triassic boundary. Australian Journal of Earth Sciences, 55(3): 365-377. https://doi.org/310.1080/08120090701769480

Meyers, W. J. ,Lohmann, K. C., 1985. Isotope geochemistry of regionally extensive calcite cement zones and marine components in Mississippian limestones, New Mexico. Carbonate Cements, 36: 223-239. https://doi.org/210.2110/pec.2185.2136.0223

Nafi, M., Xia, W. ,Zhang, N., 2006. Late Permian (Changhsingian) conodont biozonation and the basal boundary, Ganxi section, western Hubei Province, south China. Canadian Journal of Earth Sciences, 43(2): 121-133. https://doi.org/110.1139/e1105-1097

Niu, Z., Duan, Q., Xu, G., et al., 2000. Sedimentation Types and Age of the Dalong Formation in western Hubei. Journal of Stratigraphy, 24(2): 151-155. https://doi.org/110.3969/j.issn.0253-4959.2000.3902.3013 (in Chinese with English Abstract)

Orchard, M. J. ,Krystyn, L., 1998. Conodonts of the lowermost Triassic of Spiti, and new zonation based on Neogondolella successions. Rivista Italiana Di Paleontologia E Stratigrafia, 104(3): 341-368.https://doi.org/310.13130/12039-14942/15339

Perri, M. C. ,Farabegoli, E., 2003. Conodonts across the Permian-Triassic boundary in the Southern Alps. Courier Forschungs Institut Senckenberg, 245(245): 281-313

Raup, D. M. ,Sepkoski, J. J., 1982. Mass extinctions in the marine fossil record. Science, 215(4539): 1501-1503. https://doi.org/1510.1126/science.1215.4539.1501

Scotese, C. R., 2001. Atlas of Earth History. Paleomap Project of Department of Geology, University of Texas at Arlington, Arlington

Schaal, E., Clapham, M., Rego, B., et al., 2015. Comparative size evolution of marine clades from the Late Permian through Middle Triassic. Paleobiology, 42(01): 217-142. https://doi.org/ 10.1016/j.gr.2013.07.019

Schobben, M., Joachimski, M. M., Korn, D., et al., 2014. Palaeotethys seawater temperature rise and an intensified hydrological cycle following the end-Permian mass extinction. Gondwana Research, 26(2): 675-683. https://doi.org/10.1017/pab.2015.36

Sepkoski, J. J., 1981. A factor analytic description of the phanerozoic marine fossil record. Paleobiology, 7(1): 36-53. https://doi.org/10.1017/S0094837300003778

Shao, L., Zhang, P., Dou, J., et al., 2000. Carbon isotope compositions of the Late Permian carbonate rocks in southern China: their variations between the Wujiaping and Changxing formations. Palaeogeography, Palaeoclimatology, Palaeoecology, 161(1): 179-192. https://doi.org/110.1016/S0031-0182(1000)00122-X

Shen, S., 2007. The conodont species Clarkina orientalis (Barskov and Koroleva, 1970) and its spatial and temporal distribution. Permophiles, 50: 25-37

Shen, S., Wang, Y., Henderson, C. M., et al., 2007. Biostratigraphy and lithofacies of the Permian System in the Laibin-Heshan area of Guangxi, South China. Palaeoworld, 16(1): 120-139. https://doi.org/110.1016/j.palwor.2007.1005.1005

Shen, S. ,Mei, S., 2010. Lopingian (Late Permian) high-resolution conodont biostratigraphy in Iran with comparison to South China zonation. Geological Journal, 45(2-3): 135-161. https://doi.org/110.1002/gj.1231

Shen, S., Crowley, J. L., Yue, W., et al., 2011. Calibrating the End-Permian Mass Extinction. Science, 334(6061): 1367-1372. https://doi.org/10.1126/science.1213454.

Shen, S., Cao, C., Zhang, H., et al., 2013. High-resolution δ13Ccarb chemostratigraphy from latest Guadalupian through earliest Triassic in South China and Iran. Earth and Planetary Science Letters, 375: 156-165. https://doi.org/110.1016/j.epsl.2013.1005.1020

Shen, S. ,Bowring, S. A., 2014. The end-Permian mass extinction: A still unexplained catastrophe. National Science Review, 1(4): 492-495. https://doi.org/410.1093/nsr/nwu1047

Song, H., Wignall, P. B., Tong, J., et al., 2012. Geochemical evidence from bio-apatite for multiple oceanic anoxic events during Permian–Triassic transition and the link with end-Permian extinction and recovery. Earth and Planetary Science Letters, 353-354: 12-21. https://doi.org/10.1016/j.epsl.2012.1007.1005

Song, H., Wignall, P. B., Tong, J., et al., 2013. Two pulses of extinction during the Permian–Triassic crisis. Nature

Geoscience, 6: 52-56. https://doi.org/10.1038/ngeo1649
Sun, S., Li, J., Chen, H., et al., 1989. Mesozoic and Cenozoic sedimentary history of south China. Aapg Bulletin, 73:1247-1269.https://doi.org/1210.1306/1244B1244AA1214-1170A-1211D1247-8645000102C8645001865D
Sun, Y., Joachimski, M. M., Wignall, P. B., et al., 2012. Lethally hot temperatures during the Early Triassic greenhouse. Science, 338(6105): 366-370. https://doi.org/10.1126/science.1224126
Tong, J. ,Zhao, L., 2005. Triassic in Chaohu, Anhui Province, guide to the mid-symposium field excursion of the international symposium on the Triassic chronostratigraphy and biotic recovery. Albertiana, 33: 129-138
Wang, C. Y. ,Wang, Z. H., 1981. Permian conodonts from Longtan Formation and Changhsing Formation of Changxing, Zhejiang and their stratigraphical and palaeoecological significance. Seclected Papers on the 1st Convention of Micropaleontological Society of China. Science Press, Beijing. 114-120 (in Chinese with English Abstract)
Wang, G. ,Xia, W., 2004a. Upper Permian conodonts zonation and its implication in western Hubei Province. Geological Science and Technology Information, 23(4): 30-34. https://doi.org/10.3969/j.issn.1000-7849.2004.3904.3007 (in Chinese with English Abstract)
Wang, G. ,Xia, W., 2004b. Conodont zonation across the Permian-Triassic boundary at the Xiakou section, Yichang city, Hubei Province and its correlation with the Global Stratotype Section and Point of the PTB. Canadian Journal of Earth Sciences, 41(3): 323-330. https://doi.org/310.1139/e1104-1008
Wang, L., Wignall, P. B., Sun, Y., et al., 2017. New Permian-Triassic conodont data from Selong (Tibet) and the youngest occurrence of Vjalovognathus. Journal of Asian Earth Sciences, 146(Supplement C): 152-167. https://doi.org/110.1016/j.jseaes.2017.1005.1014
Wei, H., Yu, H., Wang, J., et al., 2015. Carbon isotopic shift and its cause at the Wuchiapingian-Changhsingian boundary in the Upper Permian at the Zhaojiaba section, South China: Evidences from multiple geochemical proxies. Journal of Asian Earth Sciences, 105: 270-285. https://doi.org/210.1016/j.jseaes.2015.1001.1011
Xie, S., Pancost, R. D., Huang, J., et al., 2007. Changes in the global carbon cycle occurred as two episodes during the Permian-Triassic crisis. Geology, 35(12): 1083-1086. https://doi.org/1010.1130/G24224A.24221
Yang, B., Lai, X., Wignall, P. B., et al., 2012. A newly discovered earliest Triassic chert at Gaimao section, Guizhou, southwestern China. Palaeogeography Palaeoclimatology Palaeoecology, 344-345(4): 69-77. https://doi.org/10.1016/j.palaeo.2012.1005.1019
Yazdi, M. ,Shirani, M., 2002. First Research on Marine and Nonmarine Sedimentary Sequences and Micropaleontologic Significance across Permian/Triassic Boundary in Iran (Isfahan and Abadeh). Journal of China University of Geosciences, 13(2): 172-176
Yin, H., Zhang, K., Tong, J., et al., 2001. The Global Stratotype Section and Point (GSSP) of the Permian-Triassic Boundary. Episodes, 24: 102-114
Yin, H., Jiang, H., Xia, W., et al., 2014. The end-Permian regression in South China and its implication on mass extinction. Earth-Science Reviews, 137: 19-33. https://doi.org/10.1016/j.earscirev.2013.1006.1003
Yuan, D., Shen, S., Henderson, C. M., et al., 2014. Revised conodont-based integrated high-resolution timescale for the Changhsingian Stage and end-Permian extinction interval at the Meishan sections, South China. Lithos, 204(Supplement C): 220-245. https://doi.org/210.1016/j.lithos.2014.1003.1026
Yuan, D., Shen, S., Henderson, C. M., et al., 2019. Integrative timescale for the Lopingian (Late Permian): A review and update from Shangsi, South China. Earth-Science Reviews, 188: 190-209. https://doi.org/10.1016/j.earscirev.2018.11.002
Yuan, J., Jiang, H. ,Wang, D., 2015. LST: A New Inorganic Heavy Liquid Used in Conodont Separation. Geological Science and Technology Information, 34(5): 225-230(in Chinese with English Abstract)
Zhang, K., Lai, X., Tong, J., et al., 2009. Progresses on study of conodont sequence for the GSSP Section at

Meishan, Changxing, Zhejiang Province, South China. Acta Palaeontologica Sinica, 48(3): 474-486. https://doi.org/410.3969/j.issn.0001-6616.2009.3903.3018 (in Chinese with English Abstract)

Zhang, N., Jiang, H., Zhong, W., et al., 2014. Conodont Biostratigraphy across the Permian-Triassic Boundary at the Xinmin Section, Guizhou, South China. Journal of Earth Science, 25(5): 779-786. https://doi.org/710.1007/s12583-12014-10472-12580

Zhao, J., Liang, X. ,Zeng, Z., 1978. Disscussion on the horizon of Dalong Formation. Acta Stratigraphica Sinica, 2(1): 48-54. http://ir.nigpas.ac.cn/handle/332004/335225 (in Chinese)

Zhao, L., J., O. M., Tong, J., et al., 2007. Lower Triassic conodont sequence in Chaohu, Anhui Province, China and its global correlation. Palaeogeography, Palaeoclimatology, Palaeoecology, 252(1): 24-38. https://doi.org/10.1016/j.palaeo.2006.1011.1032

Zhao, L., Chen, Y., Chen, Z., et al., 2013. Uppermost Permian to Lower Triassic conodont zonation from Three Gorges area, South China. Palaios, 28(8): 523-540. https://doi.org/510.2110/palo.2012.p2112-2107r

Zhuo, J., Wang, J., Wang, Z., et al., 2009. Sedimentary Characteristics of Late Permian in western Hubei Province and Evolution of Inter-Platform Rift. Xinjiang Petroleum Geology, 30: 300-303 (in Chinese with English Abstract)

Figure captions

Figure 1. (a) Paleogeography during the Changhsingian Stage in the Middle and Upper Yangtze Region, modified from Feng et al. (1997) and He et al. (2013); (b) Paleogeography showing the position of South China during the end-Permian extinction, modified after Scotese, 2001; (c) Distribution of deep-water environments during the Changhsingian in South China, modified from Yin et al. (2014) and Sun et al. (1989). ★location of the Shiligou section, ▲location of the Zhuqiao section. NMBY = North marginal basin of Yangtze Platform; HGGB = Hunan-Guizhou-Guangxi basin.

Figure 2. The locations of the Zhuqiao and Shiligou sections, western Hubei Province, South China. ★location of the Shiligou section, ▲location of the Zhuqiao section.

Figure 3. Photos of field outcrops and fossils at the Zhuqiao and Shiligou sections in the western Hubei Province, South China. (a) Panorama of the Zhuqiao section; (b) Lithology of bed 25 to bed 29 at Zhuqiao, insert is a dolomitic mudstone of bed 26; (c) Ophiceras in the bed 27 of Daye Fm. at Zhuqiao; (d) rugged limestone surface at the base of bed 25a of Dalong Fm. at Zhuqiao; (e) overview of the WCB at Shiligou; (f) the PTB at Shiligou.

Figure 4. Distribution of conodont fossils at Zhuqiao, Wufeng County, Yichang City, western Hubei Province, South China.

Figure 5. Distribution of conodont fossils at the Shiligou section in Xinglong Town, Fengjie County, Chongqing City, South China.

Figure 6. Changhsingian $\delta^{13}C_{carb}$ chemostratigraphy at the Zhuqiao and Shiligou sections compared with the Meishan and Shangsi records from Shen et al.(2013).

Plate 1. SEM photos of conodonts from the Zhuqiao section. All illustrations are P_1 elements, Scale bar=100 μm. 1, Clarkina guangyuanensis (Dai and Zhang, 1989), from sample ZQC-01; 2, Clarkina transcaucasica Gullo and Kozur, 1992, from sample ZQC-01; 3, Clarkina liangshanensis (Wang, 1978), sample ZQC-01; 4-25. Clarkina orientalis (Barskov and Koroleva, 1970), 4-7, sample ZQC-01,8-25, sample ZQC-08-01.

Plate 2. SEM photos of conodonts from the Zhuqiao section. All illustrations are P_1 elements, Scale bar=100 μm. 1-28, Clarkina orientalis (Barskov and Koroleva, 1970), 1-2, sample ZQC-19, 3-8, sample ZQC-20, 9-14, sample ZQC-21, 15-17, sample ZQC-22, 18-23, sample ZQC-23, 24-26, sample ZQC-24-01, 27-28, sample ZQC-25-01.

Plate 3. SEM photos of conodonts from the Zhuqiao and Shiligou sections. All illustrations are P_1 elements, Scale bar=100 μm. 1-8, Clarkina orientalis (Barskov and Koroleva, 1970), Shiligou section, 1, sample SLG-01, 2-5, sample SLG-05, 6-7, sample SLG-08-02, 8, sample SLG-11-02; 9-23. Clarkina wangi (Zhang, 1987), 9-16, Zhuqiao section, sample ZQC-25-01, 17-23, Shiligou section, 17-21, sample SLG-06-01, 22-23, sample SLG-06-02; 24-27, Clarkina subcarinata (Sweet, 1973), Shiligou section, 24-26, sample SLG-08-02, 27, sample SLG-09; 28-33, Clarkina changxingensis (Wang and Wang, 1981), Shiligou section, 28-29, sample SLG-12, 30-31, sample SLG-13-01, 32-33, sample SLG-13-02.

Plate 4. SEM photos of conodonts from the Zhuqiao and Shiligou sections. All illustrations are P_1 elements, Scale bar=100 μm. 1-5，Clarkina changxingensis (Wang and Wang, 1981), Shiligou section, 1, sample SLG-15-01, 2, sample SLG-15-02, 3-4, sample SLG-16-02, 5, sample SLG-16-03; 6, Clarkina deflecta (Wang and Wang, 1981), Shiligou section, sample SLG -15-01; 7-9, Clarkina yini Mei, 1998, Shiligou section, 7, sample SLG-15-01, 8, sample SLG-15-03, 9, sample SLG-16-02; 10-12, Clarkina meishanensis (Zhang et al., 1995), Zhuqiao section, sample ZQC-25-02; 14, 19-20. Hindeodus parvus (Kozur and Pjatakova,1976), Zhuqiao section, 14, sample ZQC-28, 19, sample ZQC-34-01, 20, sample ZQC-34-02; 13, 15, Hindeodus sp., 13, Shiligou section, sample SLG15-01, 15, Zhuqiao section, sample ZQC-28; 16, Clarkina orchard (Mei, 1996), Zhuqiao section, sample ZQC-28; 17, Hindeodus pisai Perri and Farabegoli, 2003, Zhuqiao section, sample ZQC-30-02;18, Isarcicella isarcica (Huckriede, 1958), Zhuqiao section, sample ZQC-30-02; 21. Hindeodus aff. parvus, Shiligou section, sample SLG-17-03.

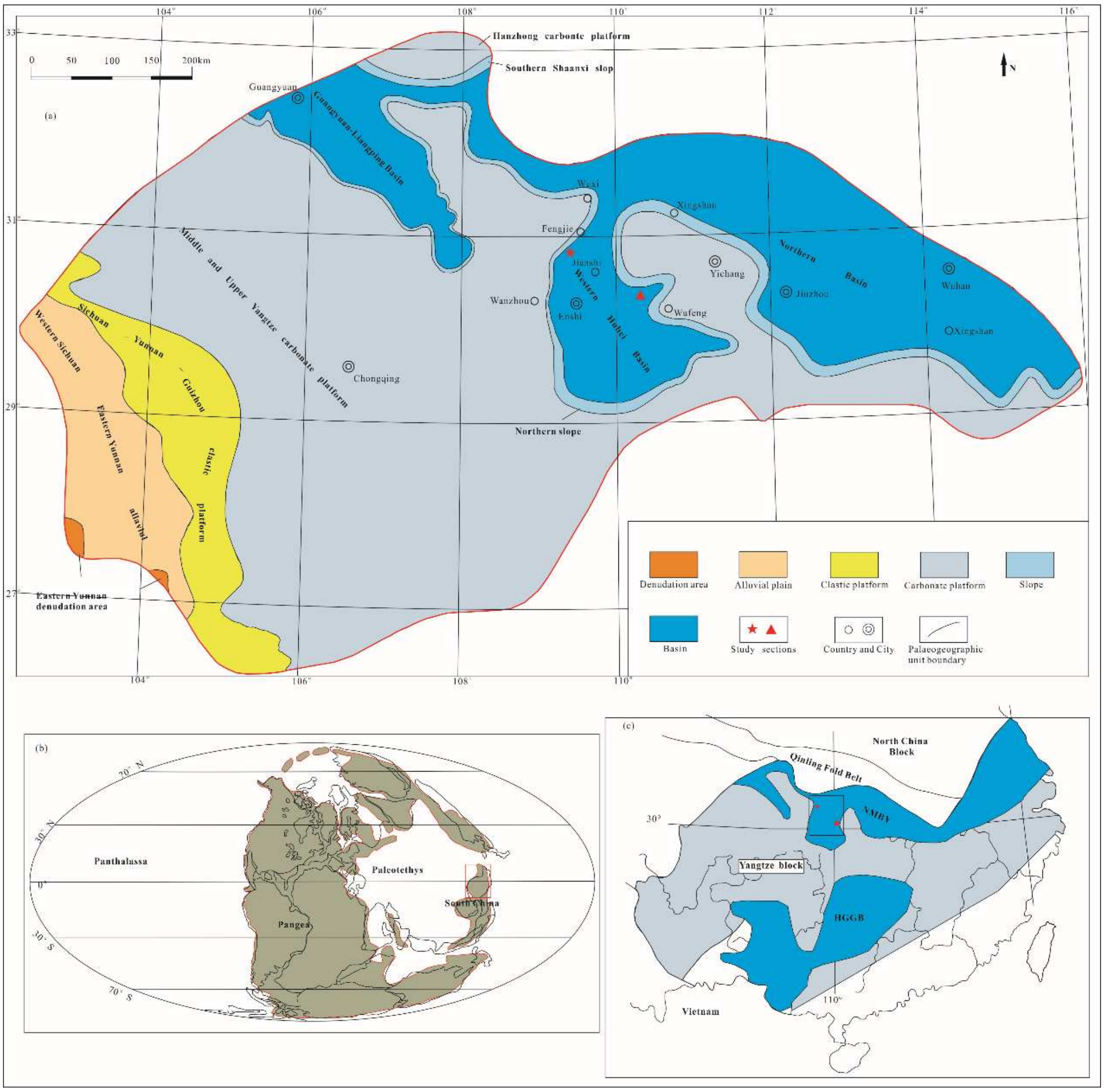
Hanzhong carbonte platform
Southern Shaanxi slop
(a)
Guangyuan
Guangyuan-Liangping Basin
Wuxi
Xingshan
Fengjie
Jianshi
Western Hubei Basin
Yichang
Wanzhou
Enshi
Wufeng
Jinzhou
Northern Basin
Wuhan
Middle and Upper Yangtze carbonate platform
Chongqing
Sichuan Yunnan Guizhou clastic platform
Western Sichuan Eastern Yunnan alluvial
Northern slope
Eastern Yunnan denudation area
Denudation area
Alluvial plain
Clastic platform
Carbonate platform
Slope
Basin
Study sections
Country and City
Palaeogeographic unit boundary
(b)
Panthalassa
Paleotethys
Pangea
South China
(c)
North China Block
Qinling Fold Belt
YMBY
Yangtze block
HGGB
Vietnam

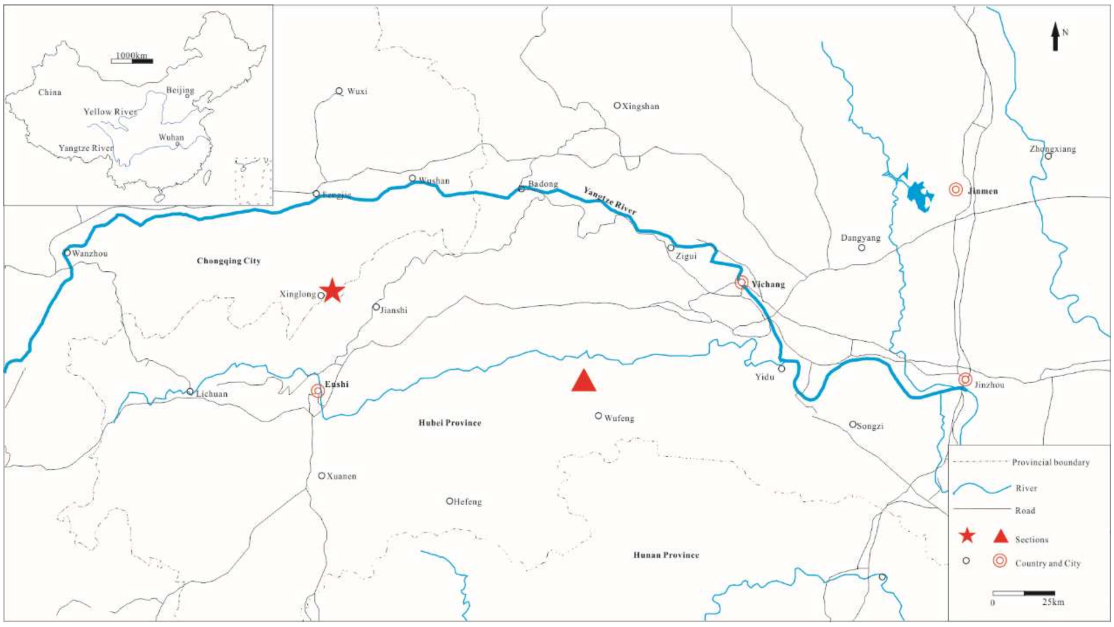
China
Beijing
Yellow River
Wuhan
Yangtze River
Wuxi
Xingshan
Zhongxiang
Fengjie
Wushan
Badong
Yangtze River
Jinmen
Wanzhou
Chongqing City
Zigui
Dangyang
Xinglong
Jianshi
Yichang
Lichuan
Enshi
Yidu
Jinzhou
Hubei Province
Wufeng
Songzi
Xuanen
Hefeng
Hunan Province
Provincial boundary
River
Road
Sections
Country and City
0
25km


Daye Fm.
Wuchiaping Fm.
Dalong Fm.
1m
(a)
Ophiceras
H.parvus
28
29
PTB
27
WCB
Dalong Fm.
25
26
Daye Fm.
(b)
25
(d)
WCB
6
5
Dalong Fm.
(e)
PTB
17
16
Daye Fm.
Dalong Fm.
(f)

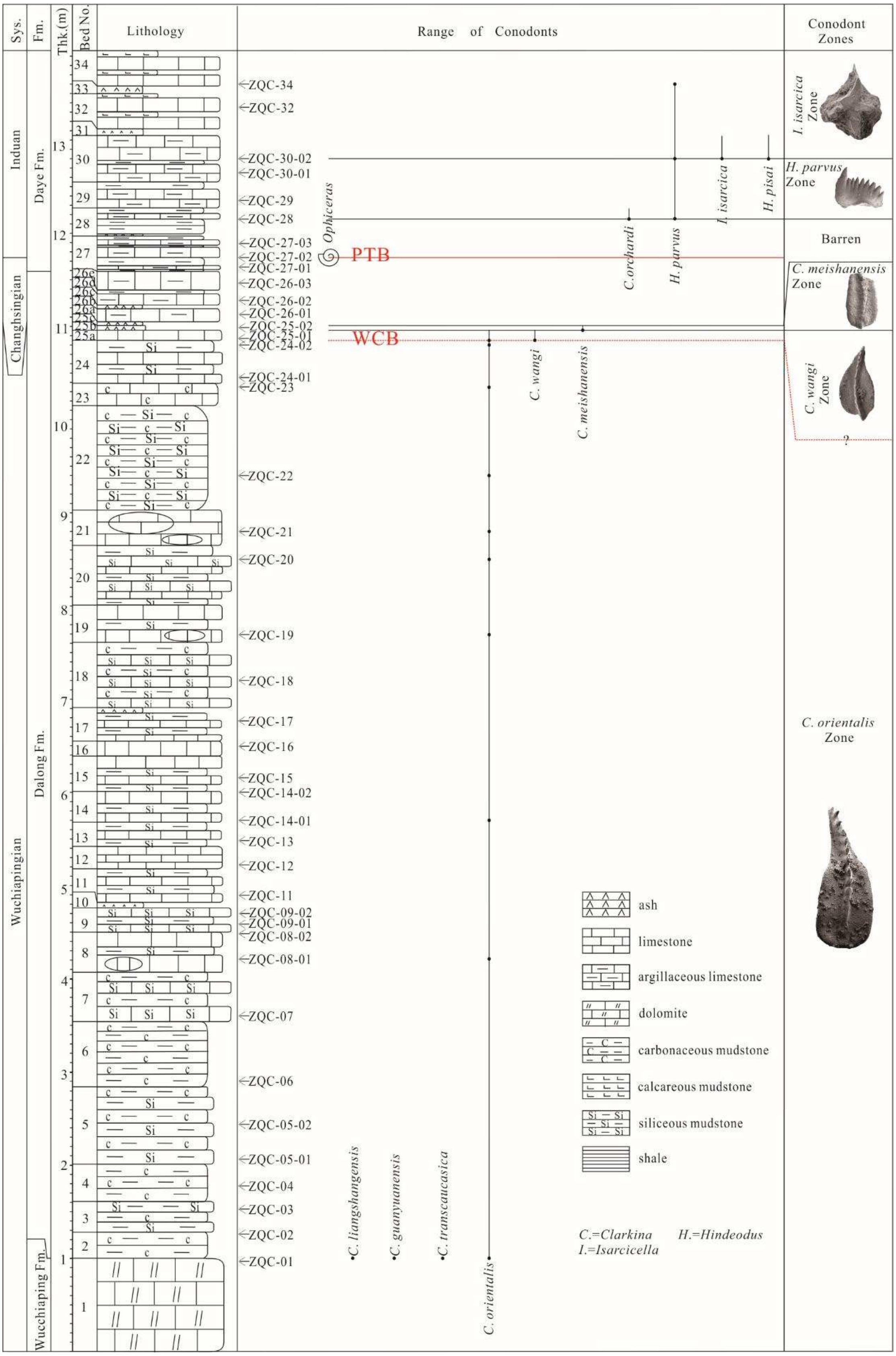

Sys.
Fm.
Thk.(m)
Bed No.
Lithology
Range of Conodonts
Conodont Zones
Induan
Daye Fm.
Changhsingian
Wuchiapingian
Dalong Fm.
Wucchiaping Fm.
ZQC-34
ZQC-32
ZQC-30-02
ZQC-30-01
ZQC-29
ZQC-28
ZQC-27-03
ZQC-27-02
ZQC-27-01
ZQC-26-03
ZQC-26-02
ZQC-26-01
ZQC-25-02
ZQC-25-01
ZQC-24-02
ZQC-24-01
ZQC-23
ZQC-22
ZQC-21
ZQC-20
ZQC-19
ZQC-18
ZQC-17
ZQC-16
ZQC-15
ZQC-14-02
ZQC-14-01
ZQC-13
ZQC-12
ZQC-11
ZQC-09-02
ZQC-09-01
ZQC-08-02
ZQC-08-01
ZQC-07
ZQC-06
ZQC-05-02
ZQC-05-01
ZQC-04
ZQC-03
ZQC-02
ZQC-01
Ophiceras
PTB
WCB
C. orchardi
H. parvus
I. isarcica
H. pisai
C. wangi
C. meishanensis
C. orientalis
C. liangshangensis
C. guanyuanensis
C. transcaucasica
I. isarcica Zone
H. parvus Zone
Barren
C. meishanensis Zone
C. wangi Zone
C. orientalis Zone
ash
limestone
argillaceous limestone
dolomite
carbonaceous mudstone
calcareous mudstone
siliceous mudstone
shale
C.=Clarkina H.=Hindeodus
I.=Isarcicella

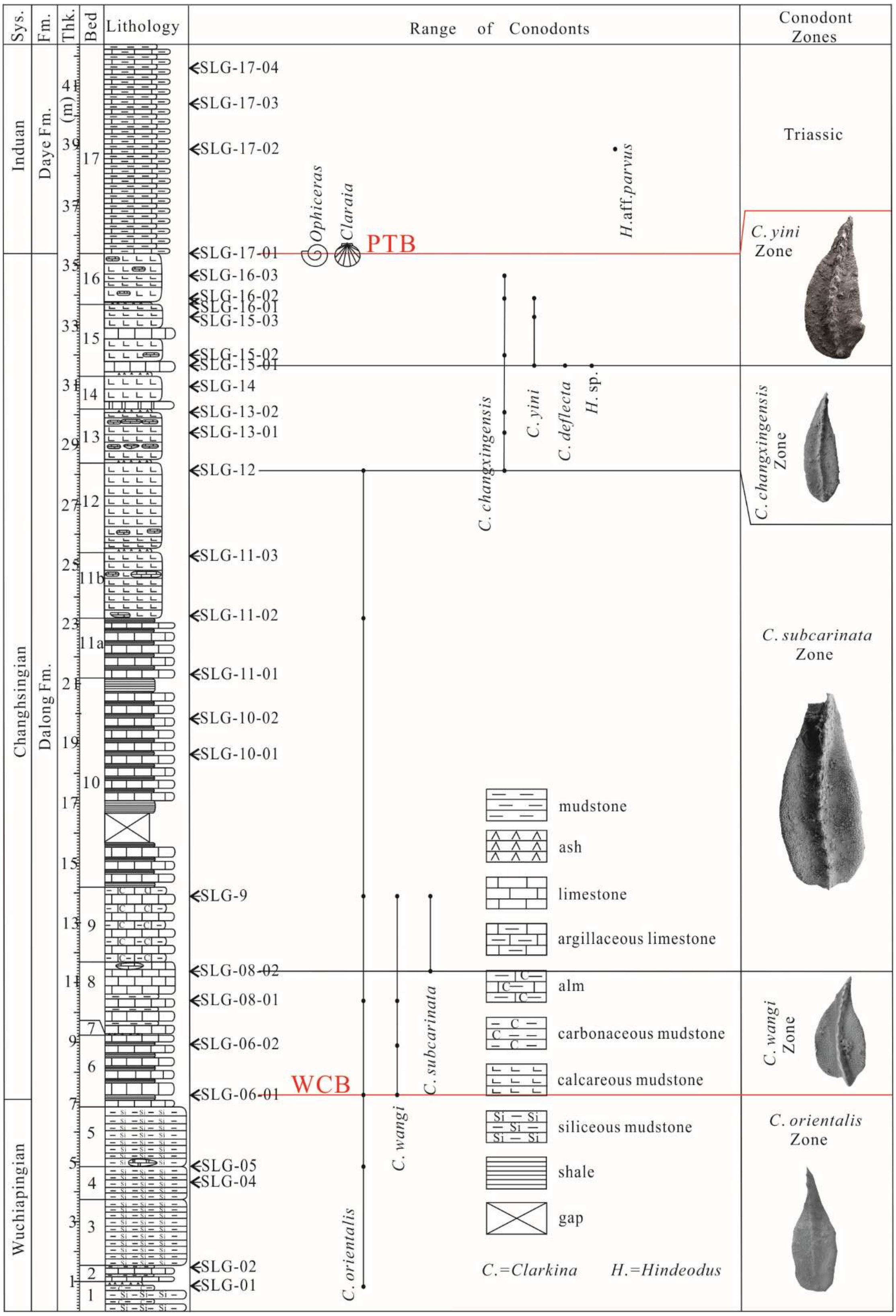
Sys.
Fm.
Thk. (m)
Bed
Lithology
Range of Conodonts
Conodont Zones
Induan
Daye Fm.
Changhsingian
Dalong Fm.
Wuchiapingian
SLG-17-04
SLG-17-03
SLG-17-02
SLG-17-01
SLG-16-03
SLG-16-02
SLG-16-01
SLG-15-03
SLG-15-02
SLG-15-01
SLG-14
SLG-13-02
SLG-13-01
SLG-12
SLG-11-03
SLG-11-02
SLG-11-01
SLG-10-02
SLG-10-01
SLG-9
SLG-08-02
SLG-08-01
SLG-06-02
SLG-06-01
SLG-05
SLG-04
SLG-02
SLG-01
Ophiceras
Claraia
PTB
WCB
H.aff.parvus
C. changxingensis
C. yini
C. deflecta
H. sp.
C. subcarinata
C. wangi
C. orientalis
Triassic
C. yini Zone
C. changxingensis Zone
C. subcarinata Zone
C. wangi Zone
C. orientalis Zone
mudstone
ash
limestone
argillaceous limestone
alm
carbonaceous mudstone
calcareous mudstone
siliceous mudstone
shale
gap
C.=Clarkina
H.=Hindeodus

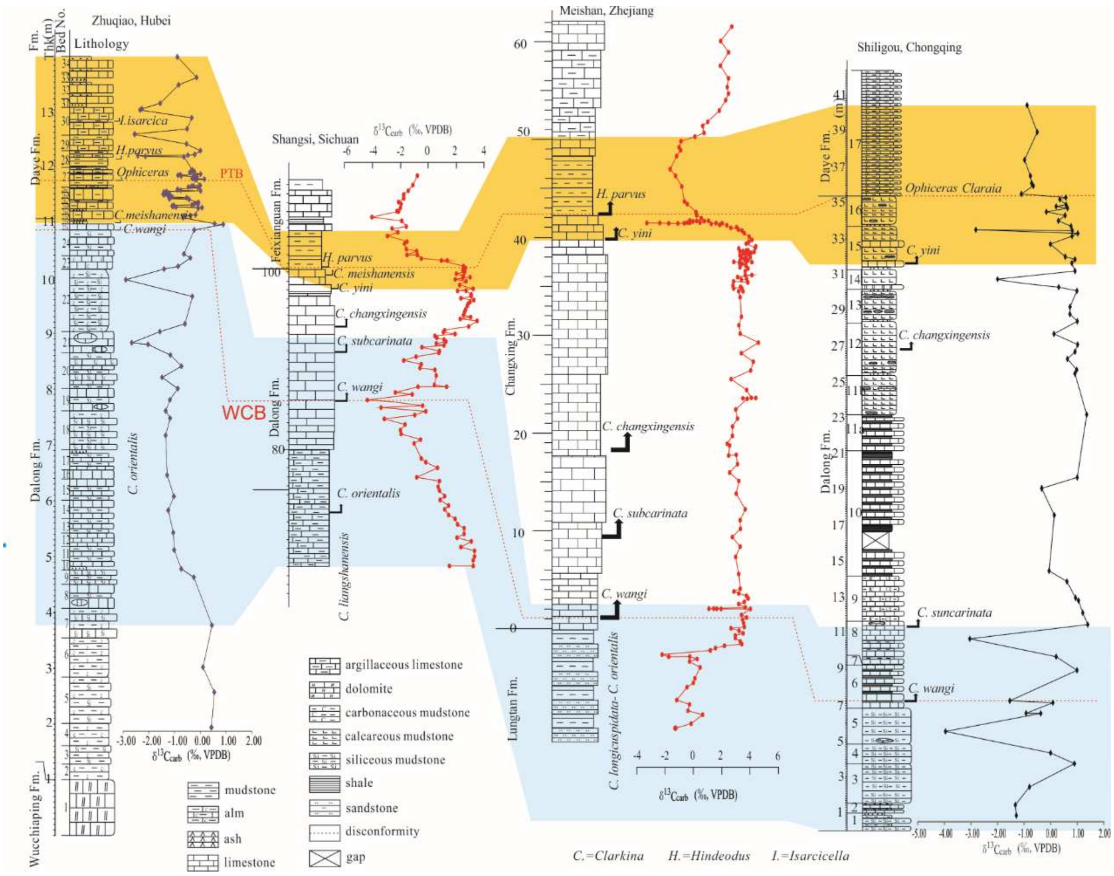

Zhuqiao, Hubei
Lithology
Fm.
Thk(m)
Bed No.
Daye Fm.
Dalong Fm.
Wuchiaping Fm.
I. isarcica
H. parvus
Ophiceras
PTB
C. meishanensis
C. wangi
C. orientalis
δ13Ccarb (‰, VPDB)
Shangsi, Sichuan
Feixianguan Fm.
Dalong Fm.
H. parvus
C. meishanensis
C. yini
C. changxingensis
C. subcarinata
C. wangi
WCB
C. orientalis
C. liangshanensis
Meishan, Zhejiang
Changxing Fm.
Lungtan Fm.
H. parvus
C. yini
C. changxingensis
C. subcarinata
C. wangi
C. longicuspidata- C. orientalis
Shiligou, Chongqing
Daye Fm.
Dalong Fm.
Ophiceras Claraia
C. yini
C. changxingensis
C. suncarinata
C. wangi
mudstone
alm
ash
limestone
argillaceous limestone
dolomite
carbonaceous mudstone
calcareous mudstone
siliceous mudstone
shale
sandstone
disconformity
gap
C.=Clarkina
H.=Hindeodus
I.=Isarcicella

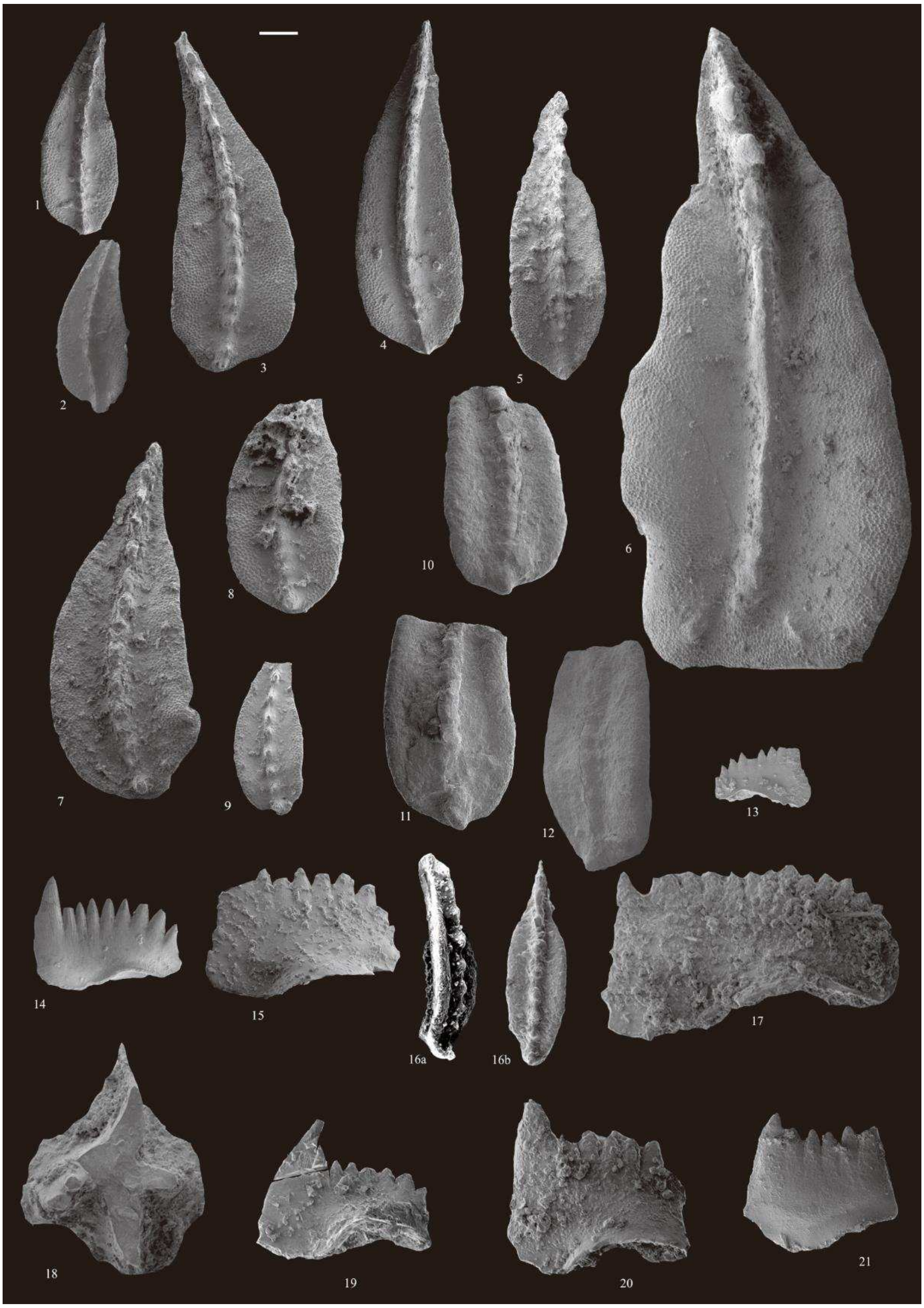

1
2
3
4
5
6
7
8
9
10
11
12
13
14
15
16a
16b
17
18
19
20
21